



# Feasibility Studies on MEMS Oxygen Flow Sensors by Differential Pressure Method for Pediatric Ventilators

M.Rajavelu<sup>1a</sup>, D.Sivakumar<sup>a</sup>, R.Joseph Daniel<sup>a</sup>,  
K.Sumangala<sup>b</sup>

<sup>a</sup>National MEMS Design Centre (NPMaSS),  
Dept. of Electronics and Instrumentation Engineering,

<sup>b</sup>Department of Civil and Structural Engineering,  
Annamalai University,

Annamalainagar – 608 002, India.

Corresponding Author : [josuma.au@gmail.com](mailto:josuma.au@gmail.com)

## Keywords:

Piezoresistive,  
ventilator system,  
pressure sensor,  
perforated diaphragm

## Abstract

This paper presents the outcome of the investigations on the measurement of oxygen flow by the differential pressure method in a pediatric ventilator system. The specialty of this flow measurement system is that it is realized using a meso channel integrated with two micro pressure sensors. The simulation results obtained from the COMSOL Multiphysics MEMS design tool show that the meso channel with a diameter of 500  $\mu\text{m}$  and a length of 20 mm can cause a measurable pressure drop between the upstream and downstream without affecting the flow. Further investigations on thin film silicon diaphragms with embedded piezoresistors for sensing upstream and downstream pressures show that it is essential to employ thin diaphragms for pressure sensing in this application to achieve higher sensitivity with reasonably good linearity. However, very thin diaphragms result in more non linearity and are difficult to realize. Hence, the authors have tried to achieve this by employing thick diaphragms but with perforations. The IntelliSuite MEMS design tool has been used to create and analyze the pressure sensors with non-perforated and perforated silicon diaphragms. The results show that it is possible to achieve more than 90% improvement in deflection and sensor sensitivities and more than 135% improvement in stress generation with a 40% perforated area irrespective of the thickness of the diaphragm. This leads to the conclusion that the perforations realized on thicker diaphragms are suitable alternatives with a more satisfactory performance than very thin non-perforated diaphragms. This work further demonstrates that it is possible to design a flow measurement system by the differential pressure method using micro sensors integrated with a meso channel.

## 1. Introduction

Recent years have been characterized by a rapid growth of interest in micro flows mainly due to the miniaturization of flow devices used for

manipulating fluids and gases in micro machines especially in the area of bio-medical engineering [Celeta et al., 2009]. Micro channels remain the most essential part of such systems. Micro channels are defined as flow passages that have hydraulic

diameters in the range of 10 to 200 micrometers. The classification of small channel dimensions classifies the range from 1 $\mu$ m to 100 $\mu$ m as micro channels, 100 $\mu$ m to 1mm as meso channels, 1mm to 6mm as compact passages, and greater than 6mm as conventional passages [Mehendale *et al.*, 2000].

Flow sensors find applications in the areas of bio-medical engineering, environmental monitoring, home appliances and industrial process control. Due to the inherent advantages of MEMS such as smaller size, higher packing density, cheaper cost, MEMS flow sensors have been developed by researchers worldwide. A sensor that translates from the physical domain to the electrical domain is needed to realize flow sensors using silicon.

There are six different techniques used to realize this sensor depending on the application of the flow sensor. The first technique uses a change in the flow induced variation of convective thermal conductance between a hot element and a fluid to measure the flow rate [Angela *et al.*, 1999]. The second method measures flow rate by measuring the heat loss due to a heating element such as a polysilicon resistor heating the fluid. This heat loss is dependent on the flow rate of the liquid and increases or decreases with the increase of flow depending on the operating mode for the structure [Angela *et al.*, 1999]. In such systems, a device that measures heat loss and translates this into the flow rate is employed. They usually suffer from non-linearity in the response and sensitivity threshold due to the transmission from free to forced convection [Angela *et al.*, 1999, Massimo *et al.*, 2009, Tae Hoon Kim *et al.*, 2009, Wiegerink *et al.*, 2009, Wu *et al.*, 2000, Yong Xu *et al.*, 2005 and Zhiyong *et al.*, 2007]. The third approach is to measure the flow by detecting the amount of heat transported by the fluid. These differential calorimetric flow sensors are usually made up of a heater positioned between an upstream and a downstream temperature probe while the output signal is the temperature difference [Paolo Bruschi *et al.*, 2005]. The fourth technique measures the time taken by a heat pulse to cover a known distance and the time of flight sensors' sensitivity is very low at small flow rates [Paolo Bruschi *et al.*, 2005].

The fifth possible method by which flow rate can be measured is by measuring differential pressure or the pressure gradient. Shear stress sensors have been used to estimate flow rate from the indirect measurement of differential pressure in terms of shear stress. This technique has reasonably good linearity over the range of flow measurements. The frictional pressure drop for liquid flow through micro channels with diameters ranging from 15  $\mu$ m to 150  $\mu$ m was explored [Judy *et al.*, 2002]. The sixth method employs a cantilever structure in the flow path and measures the deflection to measure the flow [Qi Zhang *et al.*, 2010].

Among these flow measurement techniques, viz. temperature variation in the flow channel method, the cantilever method and differential pressure methods are used to detect the flow rate widely as seen from the reported research studies. The temperature variation method is characterized by high sensitivity but it gives a non-linear output. The present research aims at achieving an accurate measurement of oxygen flow in pediatric ventilator systems. In such systems, it is essential to measure the flow rate of oxygen precisely, in addition to achieving linear output with little intervention to the flow because either over dosage or under dosage of oxygen will cause severe health hazards like suffocation. Due to a defective oxygen supply system, eleven infants died in two days due to lack of oxygen supply through ventilators in Hyderabad, Andhrapradesh [HT Correspondent, September 03, 2011, Hindustan Times, Hyderabad]. The operating range of flow rate of pediatric ventilators is from 0 to 200 ml/min. The authors propose an oxygen flow measurement system for pediatric use by employing a flow resistor in the form of a meso channel and two micro pressure sensors for measuring the upstream and downstream pressures. The flow can be characterized by the difference in upstream and downstream pressures. In the present system, a MEMS pressure sensor is used to measure the pressure which is basically composed of a diaphragm structure that converts the pressure into a linear deflection and certain sensing elements corresponding to their sensing principles, e.g., capacitive, piezoelectric or piezoresistive effects [Bernd Folkmer *et al.*, 1996, Berns *et al.*, 2006, Bhat, K.N. *et al.*, 2006, Ingelin Clausen *et al.*, 2007, Ranjit

Singh et al., 2002, Shyam Aravamudhan et al., 2008, Wisitsoraat et al., 2007 and Zhao Linin et al., 2006]. However, most of them use silicon for a diaphragm and the piezoresistive property of silicon or polycrystalline silicon as a sensing mechanism.

The present work reported in this research paper describes the design of the meso channels intended to achieve a smaller but measurable pressure drop in addition to designing appropriate pressure sensor diaphragms that detect even small variations in the upstream and downstream pressures. This requires very thin diaphragms to achieve larger sensitivity with reasonable linearity which is very difficult to realize in practical situations. Hence, it becomes essential to find suitable techniques to achieve larger deflection sensitivity with thicker diaphragms but modified to achieve larger sensitivity with reasonable linearity. One such approach that can be employed to improve sensitivity is to reduce the stiffness of thicker diaphragms by incorporating perforations in the diaphragms. Such perforated diaphragms for measuring hydrogel osmotic swelling pressures have been reported recently [Lin et al., 2010 and Orthner et al., 2010]. This paper first describes the design of meso channels for this pediatric application and then describes the research results of simulation studies on piezoresistive pressure sensors employing perforated silicon diaphragms. The deflection and sensitivities of these sensors with perforated diaphragms have been estimated and compared with sensors employing non-perforated diaphragms. Finally the authors present the oxygen flow measurement system by integrating the two units mentioned above.

## 2. Structure and Specification of a Pediatric Ventilator System

Figure 1 shows a schematic diagram of the proposed pediatric ventilator system in which the meso channel of length (L) and diameter (D) is employed to develop a nominal pressure drop and the silicon piezoresistive pressure sensors PS1 and PS2 mounted at the upstream and downstream points of the meso channel measure the pressure drop developed by the flow-resisting meso channel.

The meso channel is used as the flow resistor. Hence it is important to design the geometry of this

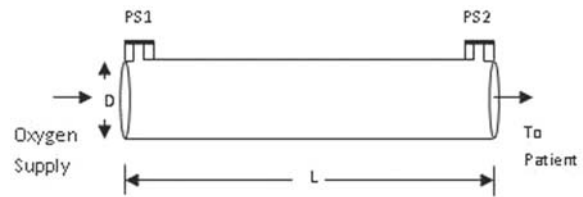


**Figure 1. Pediatric ventilator system**

channel in such a way that a sufficiently high pressure drop is achieved for the accurate measurement of differential pressure and yet does not alter the flow rate seriously. In the case of pediatric ventilators, the oxygen flow level set is from 0 to 200 ml/min. The diameter and length of the channel should be designed to satisfy this requirement. Hence, various meso channel dimensions were tried to optimize the diameter and length of the meso channel.

Table 1 shows the differential pressure ( $\Delta P$ ) for various meso channels with different lengths (L) and diameters (D). A closer look at this table indicates that the optimum dimensions of the meso channel is when  $D=50 \mu\text{m}$  and  $L=20 \text{mm}$  and whose pressure drop is 1.69 kPa which is neither low nor high, but optimum.

**Table 1. Parameters used for the study of Flow Resistor**

Sl.No.	Diameter, D	Length, L	$\Delta P$ (Pa)
1	1000 $\mu\text{m}$	20mm	80
2	500 $\mu\text{m}$	20mm	1692
3	250 $\mu\text{m}$	10mm	13538

Table 2 presents the specifications of the pediatric ventilator system proposed in this work.

**Table 2. Specification of the Ventilator System**

Parameter	Value
Length, L	20mm
Diameter, D	500 $\mu\text{m}$
Upstream Pressure, $P_1$	20 KPa
Flow Rate, FR	0 to 200 mL/min
Change in Voltage, $\Delta V$	0 to 1mV

## 3. Flow Performance of Meso Channel

Meso channels of different lengths and diameters were simulated using a COMSOL

Multiphysics tool and the optimum diameter and the length of the channel was found to be 500 $\mu$ m and 20mm respectively for the flow rate of oxygen from 0 to 200mL/min normally used for the pediatric ventilator. The Reynolds number for the considered structure and the flow condition ranges from 0 to 550 and hence it can be said to be a laminar flow. The flow performance of the meso channel described above and employed to develop the pressure drop in the ventilator system has been obtained through a COMSOL Multiphysics simulation and the results are presented in the forthcoming sections.

### 3.1 Boundary and initial conditions

In the meso channel, the inlet velocity referred to as  $U_{in}$  is defined in m/sec. This inlet velocity is calculated with the relationship  $Q=A \times V$  where 'Q' is the flow rate in m<sup>3</sup>/sec, 'A' is the area of cross-section of the flow resistor (meso channel to be 'D' = 500  $\mu$ m) and 'V' is the velocity in m/sec. The flow rate considered for the pediatric ventilator system in this work is 0 to 200 mL/min and the corresponding velocity is found to be 0 to 16.9765 m/sec which is assigned to  $U_{in}$  for analysis. The outlet parameters are pressure and no viscous stress. The slip condition at the wall of the meso channel is defined as 'No Slip'. The density of the oxygen used is 1.308 kg/m<sup>3</sup> and the dynamic viscosity is 20.18e-6 Pa.sec. These parameters are given as initial conditions before the start of the simulation using the COMSOL Multiphysics tool.

### 3.2 Simulation Results

The pressure profile of the oxygen flow along the channel for the flow ranging from 0 to 200mL/min has been obtained at different distances of the channel from upstream to downstream points and is presented in Figure 2.

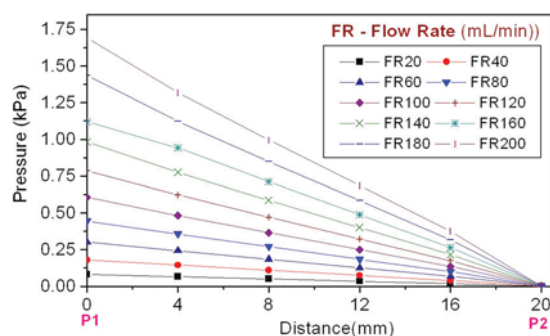


Figure 2. Pressure profile for various Flow rates

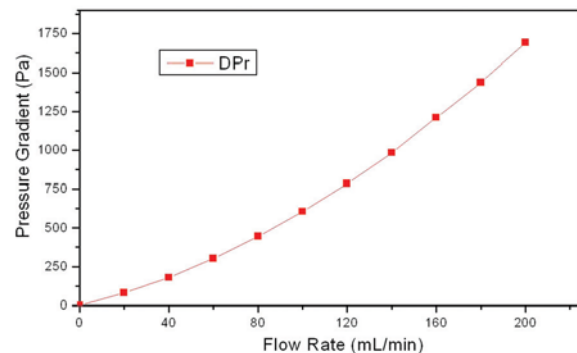


Figure 3. Flow rate Vs Pressure Gradient

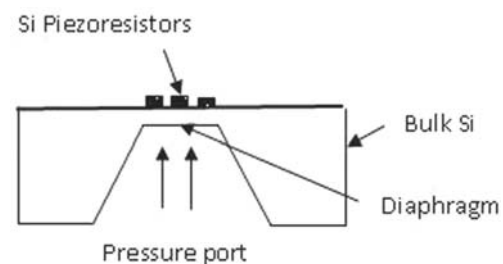


Figure 4. Structure of Silicon Piezoresistive Pressure Sensor

$P_1$  and  $P_2$  in the graph represent the upstream and downstream pressures. Figure 2 exhibits a linear variation in the pressure for the range of flow considered for the pediatric ventilator system. It is also seen from the simulation results that the pressure gradient lies in the range of 0 Pa to 1.69 kPa for the flow channel considered and this condition is presented in Figure 3.

## 4. Design and Performance Evaluation of Piezoresistive Pressure Sensor

Since the upstream pressure is fixed at 20 KPa, we should design the pressure sensors both PS1 and PS2 shown in Figure 1 such that they exhibit sensitivity and linearity over the entire operating range of 0 to 20 kPa.

### 4.1 Structure of a Silicon Piezoresistive Pressure Sensor

The cross-sectional view of two silicon piezoresistive pressure sensors PS1 and PS2 mounted on a flow resistor (meso channel) employing a silicon diaphragm to measure upstream and downstream pressures is shown in Figure 4. It is a planar silicon diaphragm formed by anisotropic etching (bulk micromachining) that converts pressure into linear deflection. The silicon substrate

at the bottom of the diaphragm provides the much needed mechanical support. It is etched partially using a bottom up approach so that a square cavity which acts as a pressure port is formed.

Three different thicknesses of square diaphragms viz.  $3\mu\text{m}$ ,  $5\mu\text{m}$  and  $7\mu\text{m}$  are considered for analysis.

#### 4.2 Simulation results of load deflection of pressure sensor

The deflection sensitivity and the sensor sensitivity for the diaphragms mentioned above for the pressure of 1 Kpa are obtained and presented in Table 3 when the bridge excitation voltage is 5V.

**Table 3. Performance of Pressure Sensors**

Sl. No.	$t_{si}$ ( $\mu\text{m}$ )	Deflection Sensitivity ( $\mu\text{m}/\text{kPa}$ )	Sensor Output @ 20 kPa(mV)
1	3	0.221	24.306
2	5	0.050	9.072
3	7	0.019	4.746

It is seen from the values presented in Table 3 that the deflection as well as voltage sensitivity for a  $3\mu\text{m}$  diaphragm is larger but may not provide satisfactory linearity over the operating pressure range of 0 to 20 kPa. The  $7\mu\text{m}$  diaphragm has a smaller deflection as well as voltage sensitivity but it may give a linear output for the entire operating range. Hence, the authors propose a different approach for getting larger sensitivity with linearity over the operating range of 0 to 20 kPa by introducing small perforations in the diaphragm.

#### 4.3 Simulation results of load deflection of pressure sensors with perforated diaphragms

Figure 5 shows the silicon piezoresistive pressure sensors PS1 and PS2 mounted on the flow resistor (meso channel) employing perforated diaphragms.

The effect of perforated diaphragms has been extensively investigated in this study by formulating 4 different levels of perforations in each group in such a way that the perforated area is 10, 20, 30

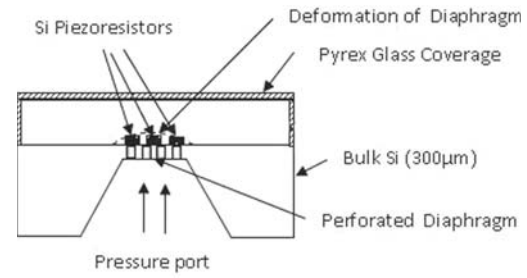


**Figure 5. Structure of Silicon Piezoresistive Pressure Sensor with Perforated Diaphragm**

and 40 percentage of the total diaphragm area. For easy reference, these devices are designated as T3-10, T3-20, T3-30 and T3-40 to indicate the 5 different levels of perforated area in the sensor group T3. The T5 and T7 group devices have also been designated using the same notations. A zero percentage perforation area refers to the non-perforated diaphragm in all these three groups which is named T3-0, T5-0 and T7-0. The diaphragm size has been chosen as  $500\mu\text{m}\times 500\mu\text{m}$  in all the 15 devices and the perforations have been symmetrically distributed so that the deflection and stress profiles resemble each other for all the diaphragms. The number of perforations varies with the percentage of the perforation area since the diaphragm size ( $500\mu\text{m}\times 500\mu\text{m}$ ) and perforation size ( $50\mu\text{m}\times 50\mu\text{m}$ ) have been kept uniform for all the cases. The shape of the perforations has been maintained as square in all the cases. The number of perforations for different devices is calculated using the equation (1).

$$N = \frac{PA}{100 \times PS} DS \quad (1)$$

Where PA is the percentage of the perforated area, DS is the diaphragm size and PS is the perforation size. The symmetrical distribution of the perforations for different perforated areas is shown in Figure 6.

In the diaphragm, perforation is achieved with the realization of etch through pores of dimension ( $50\mu\text{m}\times 50\mu\text{m}$ ) in a symmetrical fashion leaving an adequate area at the centre of the diaphragm for the placement of piezoresistors. A boron doped silicon layer of 0.6 mm thickness has been used in all the sensors considered in this study to realize the p-type piezoresistors. The dimension of all the piezoresistors implanted on the silicon diaphragm is



**Figure 6. Distribution of Perforations in the Diaphragm**

( $50\mu\text{m}\times 10\mu\text{m}\times 0.6\mu\text{m}$ ). The dimensions of these resistors have been designed in such a way that maximum sensor sensitivity is achieved [Joseph Daniel et al., 2010 and Yozo Kanda et al., 1997].

The sensitivity enhancement using perforations has been focused on in this work and in order to achieve this goal, three groups of sensors namely T3, T5, and T7 have been considered with square diaphragms of three different thicknesses ( $3\mu\text{m}$ ,  $5\mu\text{m}$  and  $7\mu\text{m}$ ). A square diaphragm for pressure sensing has been considered due to its ability to give larger sensitivity compared with a circular diaphragm [Zhao Linin et al., 2006].

Studies have been carried out using an Intellisuite MEMS design tool on the pressure sensors with both perforated and non-perforated diaphragms and it is found that the sensitivity achieved with thin non-perforated diaphragms is possible with thicker perforated diaphragms thus demonstrating that the perforated thick diaphragms are suitable alternatives to thin non-perforated diaphragms.

The IntelliSuite MEMS CAD tool has been used in this study for simulation. The structures depicted in Figure 4 and Figure 6 have been created for simulation using an Intelli FAB module. A thermo electromechanical analysis module coupled with piezoresistive analysis has been used to study the

deflection, change in resistance and sensitivity of the pressure sensor. The important parameters used in the simulation are as follows: Young's modulus of a Silicon Diaphragm = 106.8 GPa, Poisson's ratio = 0.42 and Young's modulus of a Silicon piezoresistor = 170 GPa, Poisson's ratio = 0.26. Piezoresistive Coefficients for silicon resistors:  $\pi_{11} = 6.6\times 10^{-5} \text{ MPa}^{-1}$ ;  $\pi_{12} = 1.1\times 10^{-5} \text{ MPa}^{-1}$ ;  $\pi_{44} = 95\times 10^{-5} \text{ MPa}^{-1}$ , Sheet resistance of the p-type silicon resistors =  $100 \Omega$  per square. The sensitivity of all the sensors has been estimated by operating the sensors in the small scale deflection region and hence in the linear region.

#### 4.4 Deflection responses of pressure sensors

The deflection responses have been measured in the pressure ranges of 0-1 kPa, 0-5 kPa and 0-20 kPa respectively for the device groups T3, T5 and T7 so that the deflection ( $\delta$ ) is well within the small deflection range ( $\delta < 15\%$  of diaphragm thickness) to ensure linearity. The deflection sensitivity for various perforation levels of the sensor groups T3, T5 and T7 calculated from the responses

**Table 4. Deflection Sensitivity of the Devices**

Perforated Area (%)	Deflection Sensitivity ( $\mu\text{m}/\text{kPa}$ )		
	Group T3	Group T5	Group T7
0	0.221	0.050	0.019
10	0.255	0.058	0.022
20	0.277	0.063	0.024
30	0.346	0.080	0.031
40	0.409	0.095	0.036

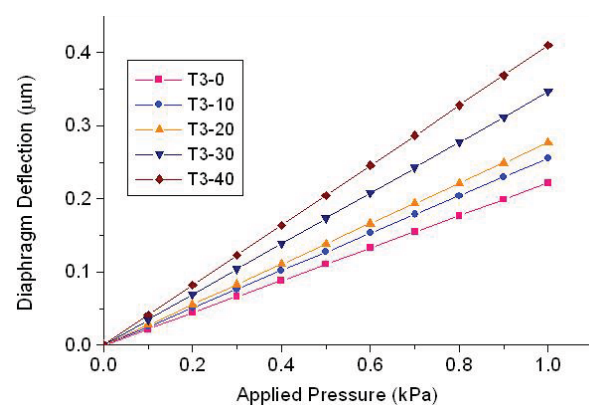


**Figure 7. Deflection responses of the Devices in T3 Group**

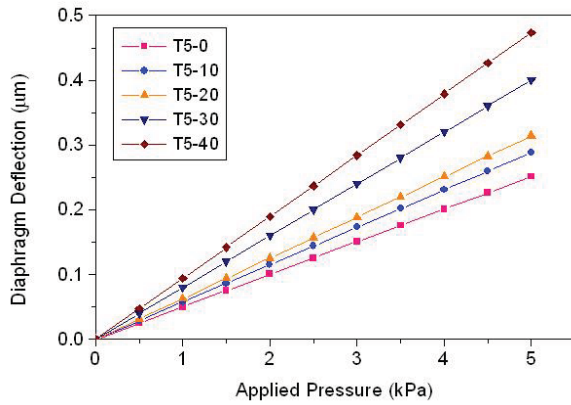


**Figure 8.** Deflection responses of the Devices in T5 Group

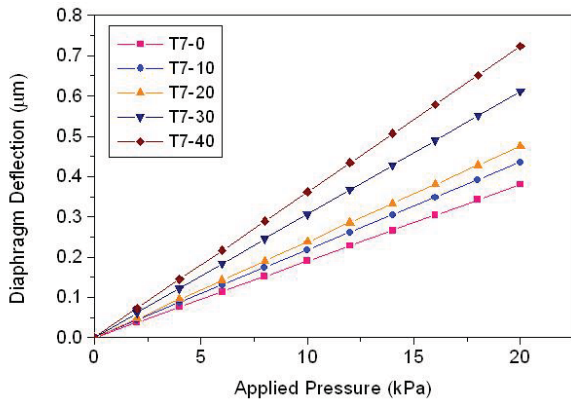


**Figure 9.** Deflection responses of the Devices in T7 Group

shown in Figures 7, 8 and 9 respectively is presented in Table 4.

It is evident from the data presented in Table 4 that the deflection sensitivity increases with an increasing percentage of perforated area irrespective of the diaphragm thickness. The percentage improvement in deflection sensitivity at various perforation levels from the non-perforated condition of the three sensor groups has been calculated and presented in Table 5. The summary of these results show that it is possible to achieve improvement to the extent of 90% with a 40 percent perforated area. The comparison of the results obtained for different groups also shows that the improvement in deflection sensitivity is almost equal for a given perforated area irrespective of the thickness. This indicates that the improvement in deflection is controlled by area rather than by volume. Since the upstream pressure for the proposed ventilator system is 20 kPa, the T7 group of sensors is able to give a linear performance in the operating range of 0 to 20 kPa.

**Table 5.** Percentage improvement in Deflection Sensitivity

Perforated Area (%)	Improvement in Deflection Sensitivity %		
	Group T3	Group T5	Group T7
0	-	-	-
10	15.38	14.83	14.45
20	25.10	24.99	25.04
30	56.52	59.38	60.88
40	85.08	88.45	90.30

#### 4.5 Stress analysis of pressure sensors and resistor size design

The piezoresistive effect is the change in resistivity of a material caused by the application of a stress. The piezoresistive coefficient relates the fractional change in resistance to the applied stress. For a diffused resistor subjected to longitudinal and transverse stress components,  $\sigma_l$  and  $\sigma_t$  respectively, the resistance change is given by equation (2).

$$\frac{\Delta R}{R} = \pi_l \sigma_l + \pi_t \sigma_t \quad (2)$$

Therefore, it becomes essential to convert the pressure into larger plane stresses for getting a larger change in resistance which will in turn result in higher output voltage. Though it has been established in the previous sections that the deflection sensitivity has been improved considerably with perforations, it becomes necessary to investigate if large stress is generated in the diaphragms on application of pressure. The longitudinal stress values measured along the Y=0 line of the diaphragm for different devices of group T3 at P=1kPa applied from the bottom of the diaphragm are shown in Figure 10.

It is evident from this graph that the stress levels increase with an increase in the perforated area at all points. The tensile stress experienced by the diaphragm at the centre increases from 3.4 MPa to 8.1 MPa and the compressive stress experienced by the diaphragm at the left and right edges increases from -5.5 MPa to -11.9 MPa when the perforated area is increased from 0 to 40% as seen in Table 6. This amounts to a 136.9% improvement

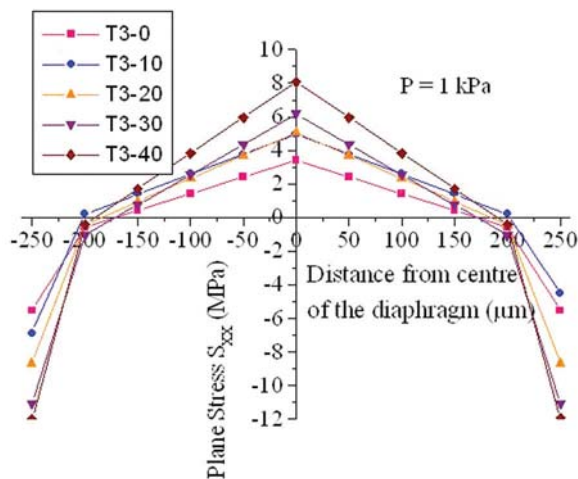


Figure 10. Longitudinal stress ( $S_{xx}$ ) measured at  $Y=0$  line

Table 6. Percentage improvement in Stress (%)

Perforated area (%)	Improvement in stress (%)	
	At midpoint	At right and left edges
0	-	-
10	45.00	24.54
20	48.74	56.75
30	81.10	100.35
40	136.6	115.89

in the tensile stress at the centre and a 115.9% improvement in the compressive stress at the diaphragm edges. This result clearly demonstrates the ability of the perforated diaphragm to generate large stresses that are essential for getting significant signals from piezoresistors.

#### 4.6 Piezoresistive analysis of pressure sensors

A Piezoresistive analysis was next carried out to measure the change in resistance on application of pressure. The voltage output obtained as differential voltage from the bridge is plotted for all the devices in groups T3, T5 and T7 in Figures 11, 12 and 13 respectively.

It is again evident from these results that the sensor output voltage increases with an increase in the perforated area. The sensor sensitivities calculated from the output voltage versus applied pressure curves presented in Figures 11, 12 and 13

for the various devices of the three groups are summarized in Table 7.

The measured change in resistance and calculated improvement in sensor sensitivity at various perforation levels of the sensors of groups T3, T5 and T7 are plotted in Figure 14. The sensor

Table 7. Measured sensor output

Perforated area (%)	Pressure Sensor output at 20 kPa (mV)		
	Group T3	Group T5	Group T7
0	24.31	9.07	4.74
10	27.91	10.48	5.49
20	29.85	11.25	5.91
30	35.42	13.61	7.21
40	42.25	16.83	9.09

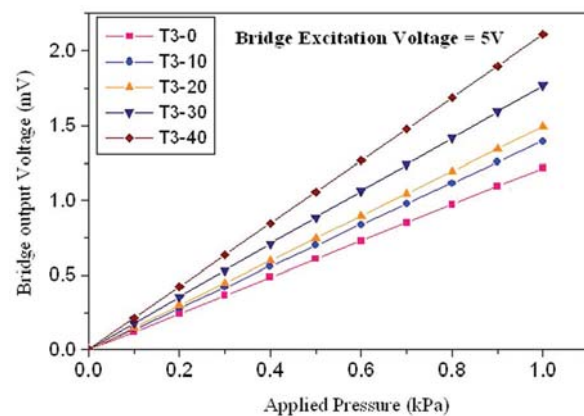


Figure 11. Output voltage versus Applied Pressure for T3 Group of Sensors

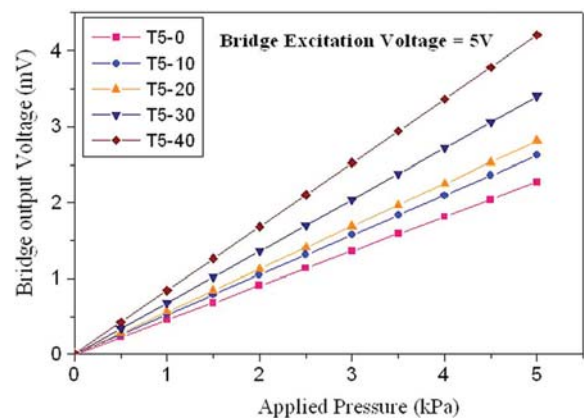


Figure 12. Output voltage versus Applied Pressure for T5 Group of Sensors



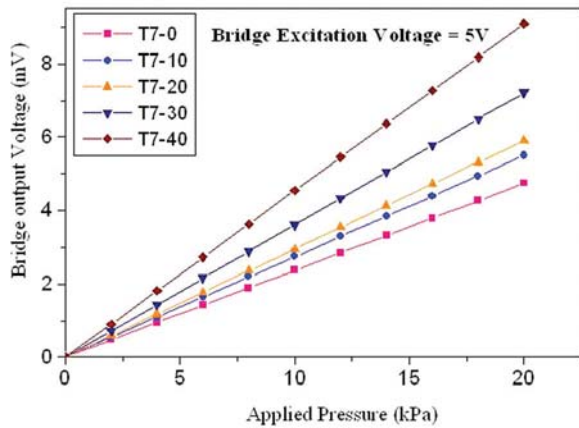


Figure 13. Output voltage versus Applied Pressure for T7 Group of Sensors

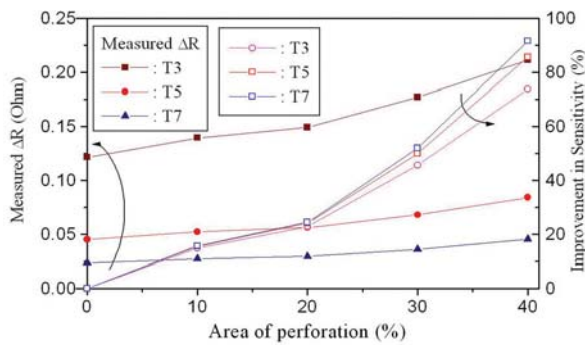


Figure 14.  $\Delta R$  and Improvement in sensitivity with perforated area

sensitivity improvement is as high as 74%, 86% and 94% in group T3, T5 and T7 respectively for a perforated area of 40%. But the sensors in the T7 group only provide linear output from 0 to 20 kPa whereas the sensors in T5 and T3 provide linearity only up to 5 kPa and 1 kPa only. Hence the T7 group of sensors only suits the need to give a satisfactory performance in the entire operating range of 0 to 20 kPa for the proposed ventilator system.

#### 4.7 Experimental validation

The sensitivity of the sensor T3-0 was reported to be  $3\mu V/V/Pa$  for an array of thirteen pressure sensors [Berns et al., 2006]. From the Intellisuite simulation results presented in Table 7, the pressure sensor output for T3-0 is 24.31 mV at 20kPa for a bridge excitation of 5V. This corresponds to  $3.16\mu V/V/Pa$  for a similar array of thirteen pressure sensors. Since the dimensions of the pressure sensor T3-0 reported in Berns et al., 2006 are the same with the simulated pressure sensor, it is concluded

that the simulation results of various perforated diaphragms presented in this study are correct.

### 5. Oxygen Flow Sensor Performance

Figure 15 shows the voltage output from the bridge circuit of the pressure sensors PS1 and PS2 by using the pressure sensor T7-40 for the upstream and downstream pressures respectively for a flow rate ranging from 0 to 200 mL/min when the bridge is excited with 5V. From this graph, it is seen that the  $\Delta V$  increases as the flow rate increases.

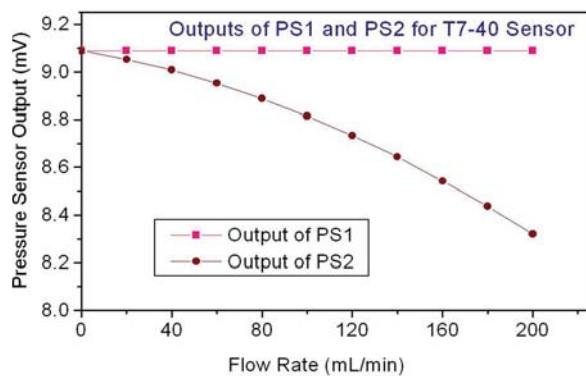


Figure 15. Flow Rate Vs Pressure Sensor Output

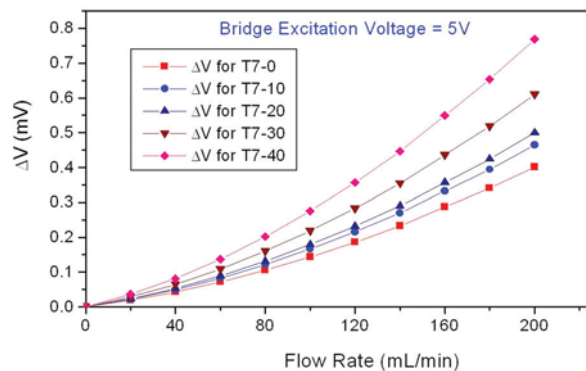


Figure 16. Flow Rate Vs Change in Voltage,  $\Delta V$

Figure 16 shows the relationship between the flow rate and the change in voltage,  $\Delta V$  obtained for the pressure drop developed by the two pressure sensors PS1 and PS2 by using all the sensors of group T7 when the upstream pressure is 20 kPa and the bridge excitation voltage is 5V.

It is observed from the graph that the pressure sensor T7-40 is the most sensitive of the sensors in the T7 group and provides good linearity. Hence, this sensor can satisfy the design specification of

the proposed ventilator system for the measurement of the oxygen flow rate. The output of this sensor is 9.09 mV for a maximum flow rate of 200 mL/min.

## 6. Conclusions

The authors report the design of a MEMS oxygen flow sensor using the differential pressure method. The optimum dimension of meso channels that give the required flow resistance was obtained from the COMSOL Multiphysics simulation. It has been found that the pressure drop is 1.69 kPa at 200 mL/min. Hence, the design should aim at achieving better sensitivity in the operating range of 0 to 20 kPa with the piezoresistive pressure sensor. However, it was found that silicon diaphragms of smaller thickness can give greater sensitivity but poor linearity in the operating range. Hence, the feasibility of achieving greater sensitivity with reasonably good linearity with perforated silicon diaphragms was investigated. Three group of devices with 3,5 and 7 $\mu$ m silicon diaphragm thickness without perforation as well as with perforations in different percentages of 10, 20, 30 and 40 were considered for the investigation. Out of all the 15 sensors, the sensor T7-40 was found to be giving a linear output over an operating range of 0 to 20 kPa with a voltage output of 9.09 mV which is almost double that of the output of the T7-0 sensor when the bridge excitation voltage is 5V for 20 kPa pressure. The results also show that the meso channel integrated with the pressure sensors can measure the oxygen flow in the pediatric ventilator system satisfactorily.

Further, a comparison of the sensor sensitivity obtained for the devices T5-0 and T7-40 (90 $\mu$ V/V/kPa) reveals that it is possible to achieve the sensitivity obtained with thin non-perforated diaphragms with thicker perforated diaphragms thus demonstrating that the perforated thick diaphragms are suitable alternatives to thin non-perforated diaphragms.

## Acknowledgement

The authors express their sincere gratitude to Prof. K.N. Bhat for teaching us the concepts of MEMS. The authors express their sincere gratitude to the NPMaSS authorities for the MEMS

Simulation and Design tools provided to NPMaSS MEMS Design Centre - Annamalai University.

## References

- Aravamudhan S., and Bhansali, S., 2008, Reinforced piezoresistive pressure sensor for ocean depth measurements, *Sensors and Actuators A*, 142: 111–117.
- Berns, A., Buder, U., Obermeier, E., Wolter, A., and Leder, A., 2006, Aero MEMS sensor array for high-resolution wall pressure measurements, *Sensors and Actuators A*, 132: 104–111.
- Bruschi, P., Diligenti, A., Navarrini D., and Piotto, M., 2005, A double heater integrated gas flow sensor with thermal feedback, *Sensors and Actuators A*, 123-124: 210-215.
- Celata, G.P., Lorenzina, M., Morini, G.L., and Zummo, G., 2009, Friction factor in micropipe gas flow under laminar, transition and turbulent flow regime, *International Journal of heat and fluid flow*, 30: 814–822.
- Clausen I. and Sveen, O., 2007, Die separation and packaging of a surface micromachined piezoresistive pressure sensor, *Sensors and Actuators A*, 133: 457–466.
- Folkmer, B. Steiner P., and Lang, W., 1996, A pressure sensor based on a nitride membrane using single-crystalline piezoresistors, *Sensors and Actuators A*, 54: 488-492.
- Joseph Daniel, R, Pravin Raj, T., Narayanaswamy, M., and Sumangala, K., 2010, Piezoresistor size effect on sensitivity of SOI Piezoresistive Pressure Sensor, Fourth ISSS National Conference on Microsystems, Smart Materials, Structures, ISSS-2010, 1-4.
- Judy, J., Maynes, D., Webb, B.W., 2002, Characterization of frictional pressure drop for liquid flows through microchannels, *International Journal of Heat Mass Transfer*, 45: 3477-3489.
- Kanda Y. and Yasukawa, A., 1997, Optimum design considerations for silicon piezoresistive pressure sensors, *Sensors and Actuators A*, 62: 539-542.
- Kim, T.H., Kim, D.-K., and Kim, S.J., 2009, Study of the sensitivity of a thermal flow sensor, *International Journal of Heat Mass Transfer*, 52: 2140-2144 .
- Lin, G., Chang, S., Hao, H., Tathireddy, R., Orthner, M., Magda, J., and Solzbacher, F., 2010, Osmotic swelling

- pressure response of smart hydrogels suitable for chronically implantable glucose sensors, *Sensors and Actuators B*, 144: 332-336.
- Linin, Z., Chen X., and Guangdi, S., 2006, Analysis for load limitation of square-shaped silicon diaphragms, *Solid-State Electronics*, 132: 104-111.
- Mehendale, S.S., Jacobi, A.M., and Shah, R.K., 2000, Fluid flow and heat transfer at micro- and meso-scales with applications to heat exchanger design, *Applied Mechanics Review*, 53: 175-193.
- Oosterbroek, R.E., Lammerink, T.S.J., Berenschot, J.W., Krijnen, G.J.M., Elwenspoek, M.C. and Van den Berg, A., 1999, A micromachined pressure/flow-sensor, *Sensors and Actuators A*, 77: 167-177.
- Orthner, M., Rieth, L., Buetefisch, S., and Solzbacher, F., 2010a, Hydrogel based piezoresistive sensor arrays (2x2) for metabolic monitoring (in vitro), *Sensors and Actuators B*, 145: 807-816.
- Orthner, M., Rieth, L., Buetefisch, S., and Solzbacher, F., 2010b, Design, simulation and optimization of a novel piezoresistive pressure sensor with stress sensitive perforated diaphragm for wet sensing and hydrogel applications, *Sensors and Actuators A*, 161: 29-38.
- Piottoa, M., Dei, M., and Bruschi, P., 2009, Low pressure drop, CMOS compatible liquid flow sensor with sub ml/h resolution, *Procedia Chemistry*, 1: 96-99.
- Rasmussen A. and Zaghloul, M.E., 1999, The design and fabrication of microfluidic flow sensors, *Proceedings of the 1999 IEEE International Symposium on Circuits and Systems, ISCAS '99*. 5: 136-139.
- Singh, R., Ngo, L.L., Seng H.S., and ChweeMok, F.N., 2002, A Silicon Piezoresistive Pressure Sensor, *Proceedings of the First International Workshop on Electronic Design, Test and Applications*.
- Sivakumar, K., Dasgupta, N. and Bhat, K.N., 2006, Sensitivity enhancement of polysilicon piezoresistive pressure sensors with phosphorous diffused resistors, *Journal of Physics: Conference Series*, 34: 216-221.
- Tan, Z., Shikida, M., Hirota, M., Xing, Y., Sato, K., Iwasaki T., and Iriye, Y., 2007, Characteristics of on-wall in-tube flexible thermal flow sensor under radially asymmetric flow condition, *Sensors and Actuators A*, 138: 87-96.
- Wiegerink, R.J., Lammerink, T.S.J., Dijkstra, M., and Haneveld, J., 2009, Thermal and Coriolis type micro flow sensors based on surface channel technology, *Proceedings of the Eurosensors XXIII conference*, Elsevier, *Procedia Chemistry* 1: 1455-1458.
- Wisitsoraat, A., Patthanasetakul, V., Lomas, T., and Tuantranont, A., 2007, Low cost thin film based piezoresistive MEMS tactile sensor, *Sensors and Actuators A*, 139: 17-22.
- Wu, S., Lin, Q., Yuen, Y., and Tai, Y.C., 2000, MEMS Flow sensors for nano-fluidic applications, 13<sup>th</sup> Annual International Conference on Micro Electro Mechanical Systems, *MEMS 2000*, 745-750.
- Xu, Y., Chiu, C.-W., Jiang, F., Lin, Q., Tai, Y.-C., 2005, A MEMS multi-sensor chip for gas flow sensing, *Sensors and Actuators A*, 121: 253-261.
- Zhang, Q., Ruan, W., Wang, H., Zhou, Y., Wang, Z., and Liu, L., 2010, A self-bended piezoresistive microcantilever flow sensor for low flow rate measurement, *Sensors and Actuators A*, 158: 273-279.

**M.Rajavelu** obtained a Bachelor's degree in Electronics & Instrumentation Engineering at Annamalai University, India in 1997. He joined as Lecturer in Electronics & Instrumentation Engineering in the same University in 2000. Later he obtained a Master's in Process Control & Instrumentation Engineering in 2005 from the same University and is currently pursuing his Ph.D programme in the area of Process Control and MEMS. Presently he is an Assistant Professor in Electronics & Instrumentation Engineering at Annamalai University. He is a life member of ISSS.



**Dr.D.Sivakumar**, a Professor in the Department of Electronics & Instrumentation Engineering, Annamalai University, India has a teaching experience of more than 27 years. He obtained both B.E. (Electronics & Instrumentation) and M.E. (Power Systems) degrees from Annamalai University. Further, he completed his PhD Research programme at the PSG College of Technology, Bharathiar



University, Coimbatore. His research interests include Control System, Process Control, Fault Tolerant Control, Signal & Image Processing, Adaptive control, System identification and MEMS. He has successfully guided six PhD scholars to date. He has to his credit research papers presented in many National and International conferences and published in National as well as International Journals. He is a life member in professional bodies like ISTE and the System Society of India.

**Dr.R. Joseph Daniel** was born in 1967. He received a B.E (Electronics and Communication) from the Government College of Engineering in Tirunelveli, India and an M.E. (Communication Engg.) from the Birla Institute of Technology (BIT) in Ranchi, India in 1988 and 1993 respectively. He received a Ph.D in Electrical Engineering from IIT Madras in 2006. After serving at BIT Ranchi for 4 years from 1992 as a faculty member, he joined Annamalai University as Lecturer in 1995. Currently he is an Associate Professor in Electronics and Instrumentation Engineering Department at Annamalai University. He is also serving as the coordinator of the National MEMS design centre



established by him at Annamalai University through the NPMaSS program and the chief investigator of a UGC major research project aiming at the development of SHM techniques using MEMS accelerometers. His research interests include semiconductor devices, PSOI MOSFETs, MEMS, nanoelectronics, embedded systems. He is an active member of ISSS. He has 6 Ph.D scholars and one Ph.D scholar as a co-guide.

**Dr.K. Sumangala** received a B.E. (Civil Engineering) from P.S.N.A College of Engineering, India in 1988. After working in the construction industry for more than two years and teaching in a polytechnic for about five years, she proceeded to receive an M.E and Ph.D in Structural Engineering from Annamalai University, India. Her Ph.D research work was on damage assessment and structural health monitoring of prestressed beams using non destructive testing and artificial neural networks. She joined as Lecturer in the Department of Civil and Structural Engineering, Annamalai University in the year 2006 and his presently working in the areas of structural health monitoring, micro-structures and micromechanics.

